



# Carbon dots synthesized from *Hibiscus Tiliaceus L.* leaves via microwave-assisted methods as a photocatalyst for sustainable organic transformation

N. A. Humaera<sup>1</sup> · B. Armynah<sup>1</sup> · D. Tahir<sup>1</sup>

Received: 19 June 2023 / Revised: 2 June 2024 / Accepted: 11 June 2024

© The Author(s) under exclusive licence to Iranian Society of Environmentalists (IRSEN) and Science and Research Branch, Islamic Azad University 2024

## Abstract

In the field of nanotechnology, carbon dots (CDs) are gaining prominence as eco-friendly photocatalysts for wastewater treatment applications owing to their high water solubility, good chemical stability, and photostability. In this research, CDs were synthesized from fresh and dried Waru (*Hibiscus Tiliaceus L.*) leaves through microwave treatment for 50 min and 60 min. The synthesized CDs were analyzed through ultraviolet–visible (UV–vis) spectrophotometry and Fourier transform infrared spectroscopy, and the results revealed an absorbance peak in the wavelength range of 300–340 nm.  $n-\pi^*$  bonds in the form of C=O and  $\pi-\pi^*$  bonds in the form of C=C were attached to the surface state of CDs. Irradiation using a halogen lamp successfully enhanced the absorption properties of CDs as a photocatalyst, indicated by a decrease in the absorption peak of the UV–vis spectra. CDs synthesized from dry leaves through microwave treatment for 60 min exhibited an excellent pollutant-degradation efficiency of 87%, with an irradiation time of 30 min, while the fresh leaf-derived sample exhibited a degradation efficiency of 75%, with an irradiation time of 60 min. CDs derived from Waru (*Hibiscus Tiliaceus L.*) leaves present a new carbon source with high potential for eco-friendly wastewater treatment applications.

**Keywords** Surface state · Waru leaves · Irradiation · Wastewater treatment · Microwave-assisted method (MAM)

## Introduction

In recent years, industrial development has increased globally, particularly in the textile industries, driven by the growing human population and changing lifestyles. However, this growth has negatively impacted the environment owing to the disposal of untreated liquid waste (Haryono et al. 2018). Textile waste is one of the most common types of liquid waste. Generally, the liquid waste from textile industries contains dyes such as Congo red (CR), methyl orange, methylene blue, and azo dye, all of which are harmful to living organisms and the environment (Sausan et al. 2021). CR, in particular, is highly toxic in aquatic environments, posing a threat to various species (Saraswati et al. 2015) and causing liver, kidney, and nerve damage in humans (Januariawan

et al. 2019). Therefore, efforts are needed to minimize environmental pollution from textile waste.

Photocatalysis is one of the easiest and most effective methods for treating textile wastewater. The photocatalytic process occurs when certain materials are exposed to light irradiation. In the photocatalysis system, the generation of electrons and holes is crucial for producing free radical atoms, which are used to break the bonds of pollutant molecules. Electrons in the valence band (VB) gain energy from the irradiation, allowing them to jump or become excited to the conduction band (CB), leaving holes in the VB. These electrons and holes then react with certain molecules in the water ( $O_2$  or  $H_2O$ ) to produce free radicals that are useful for decomposing organic pollutants (Aliah et al. 2012).

Carbon dots (CDs) exhibit good photocatalytic activity in the degradation of textile wastewater owing to their strong visible light absorption, high luminescence, and excellent light-capturing ability, making them suitable for light-emitting diode (LED) applications (Sawalha et al. 2021). Additionally, they are eco-friendly and possess good water solubility (Mondal et al. 2019). CDs with good water solubility emit bright fluorescence when exposed to light and possess

Editorial responsibility: Samareh Mirkia.

✉ D. Tahir  
dtahir@fmipa.unhas.ac.id

<sup>1</sup> Department of Physics, Hasanuddin University, Makassar 90245, Indonesia



excellent optical stability, making them suitable for various applications such as sensors, bioimaging, nanomedicine, and LEDs (Yang et al. 2020). Figure 1 illustrates the various applications of CDs and the processes within CDs when they absorb energy from light for hydrogen production.

CDs synthesized from organic compounds in the form of natural resources are rich in heteroatoms, making them suitable as antibacterial agents without the need for additional external heteroatoms (Vikneswaran et al. 2014). These natural resources are typically derived from various parts of plants, including leaves, roots, peels, fibers, and flowers.

Waru leaves (*Hibiscus Tiliaceus L.*) are a source of bioactive metabolites and antioxidants, including alkaloids, flavonoids, glycosides, tannins, carbohydrates, steroids, amino acids, saponins, and proteins (Nasrollahzadeh et al. 2018; Rawool and Parulekar 2019; Andriani et al. 2017). These compounds are similar to those found in previous studies on the formation of CDs from banana peels (Atchudan et al. 2021). Additionally, the various functional groups present, such as carboxyl, hydroxyl, and amine, can easily attract cationic ions, making them potential candidates for water and wastewater treatment (Remli and Aziz 2020).

Since the discovery of CDs, microwave-assisted synthesis methods have been the most reported owing to their simplicity, cost-effectiveness, and eco-friendly nature, as they do not require additional chemicals. The microwave-assisted method (MAM) is favored because it involves low production costs, making it suitable for both small- and large-scale industries to use for treating their organic waste. Architha

et al. (2021) synthesized CDs from *Plectranthus amboinicus* (*Mexican Mint*) leaves using the MAM, resulting in spherical CDs with an average diameter of  $2.43 \pm 0.02$  nm and surface functional groups containing oxygen. The functional groups are useful in increasing water solubility (Architha et al. 2021). This method is widely used by researchers on natural carbon sources, including lotus roots (Gu et al. 2016), *Hibiscus rosa* (Suhail et al. 2020), *Nerium oleander* (Simsek et al. 2019), and raw cashew gum (Pires et al. 2015). Despite the potential of CDs as eco-friendly photocatalysts for wastewater treatment, there is a need for a sustainable and efficient synthesis method to enhance their photocatalytic performance. Additionally, exploring unconventional carbon sources for CD synthesis is crucial for expanding the range of available materials in nanotechnology applications. Table 1 presents various synthesis methods and carbon sources used in producing CDs.

The synthesis of CDs from Waru (*Hibiscus Tiliaceus L.*) leaves as a natural carbon source through the MAM for photocatalyst applications under halogen lamp irradiation has not been reported yet. The impact of halogen lamp irradiation at different durations (50 and 60 min) on the absorption properties of CDs needs to be determined to identify the most effective synthesis conditions and enhance their performance as photocatalysts. Hence, in this study, CDs from both fresh and dried Waru (*Hibiscus Tiliaceus L.*) leaves were synthesized through the MAM and applied as photocatalysts using CR as a pollutant model for textile industries. The study investigated varying irradiation times to achieve

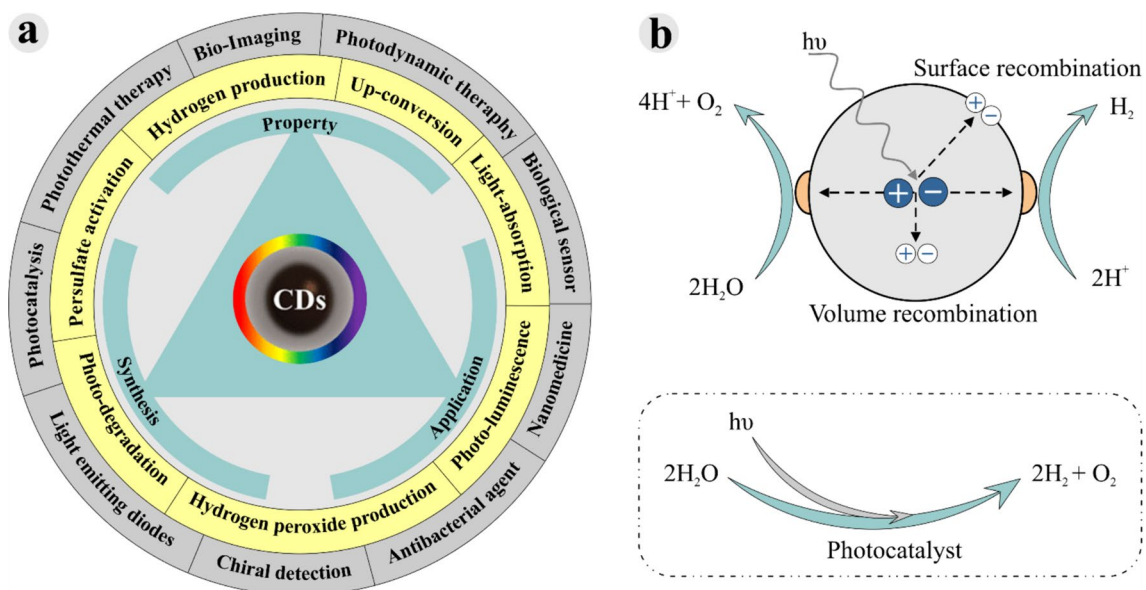


**Fig. 1** **a** Dependence of CDs on the synthesis process, which affects the applications of the CDs, including energy production (such as hydrogen and hydrogen peroxide production), electronics (such as light-emitting diodes and sensors), and medical uses (such as photo-

dynamic and photothermal therapy, nanomedicine). **b** Photocatalytic process: incoming photons (light) excite charges, initiating the reaction process for hydrogen production



**Table 1** Various synthesis methods and carbon sources used in producing CDs for photocatalysts

Synthesis methods of CDs	Carbon source	Pollutant	Light source	Time / degradation (%)	Refs.
Ultrasonication	<i>Elettaria cardamomum</i> leaves	MB and CR	Halogen 300 W	55 and 50 min/N(A)	(Zaib et al., 2021)
One pot ultrasonic	<i>Polyalthia longifolia</i> leaves	MB and CR	Halogen 100 W	60 and 90 min/N(A)	(Zaib et al., 2023)
Hydrothermal treatment	Watermelon rinds	MO	Halogen 500 W	120 min/68.941	(Remli and Aziz 2020)
Pyrolysis and chemical oxidation	Olive oil	MB	Lamp 50 W	120 min/92	(Sawalha et al. 2021)
Hydrothermal and microwave treatment	Soyabean deoiled cake	Glycerol	Mercury visible light lamp 250 W	12 h for hydrothermal and 10 min for microwave /78.7%	(Kumbhar and De 2023)
Hydrothermal treatment	3.72 g Zn(NO <sub>3</sub> ) <sub>2</sub> ·6H <sub>2</sub> O and 1.47 g C <sub>6</sub> H <sub>5</sub> Na <sub>3</sub> O <sub>7</sub> ·2H <sub>2</sub> O	MB	visible light irradiation	30 min/80	(Widiyandari et al. 2023)
Microwave-assisted	Mexican mint extract	Fe <sup>3+</sup>	UV irradiation	-	(Architha et al. 2021)

The table includes the types of dyes, types of pollutants, light sources used in the experiments, irradiation times, and degradation efficiencies



optimal efficiency. The performance of the photocatalyst was determined through kinetic model analysis using ultraviolet–visible (UV–vis) spectra recorded during halogen lamp irradiation with a wavelength range of 340–850 nm. To elucidate the structural and absorption properties of the photocatalysts, chemical functional groups were analyzed to identify  $n-\pi^*$  and  $\pi-\pi^*$  bonds at the surface state of CDs through Fouriertransform infrared (FTIR) spectroscopy. We explored the mechanism of the CD function in the photocatalyst system and demonstrated the potential eco-friendly wastewater treatment applications of CDs derived from Waru leaves by assessing their photocatalytic degradation efficiency.

The research addresses challenges associated with eco-friendly photocatalysts by focusing on the synthesis and characterization of CDs derived from Waru leaves, aiming to enhance their performance for wastewater treatment applications.

## Materials and methods

### Materials

Waru leaves (*Hibiscus Tiliaceus L.*) were collected from Tanjung Merdeka, Makassar City, South Sulawesi, and used as a carbon source. Aquades was used as a solvent, and CR served as a model organic pollutant from the textile industry.

### Preparation of waru leaves (*Hibiscus Tiliaceus L.*)

Waru leaves (*Hibiscus Tiliaceus L.*) were prepared in two forms: fresh and dried. The Waru leaves were washed thoroughly with clean water to remove dust and unwanted particles present on the surface. The dried leaves were prepared via shade -drying. The leaves were cut into small pieces and weighed using an analytical balance, with 3 g dissolved in 100 mL of distilled water each in a beaker glass. The mixing process was conducted using a blender until the solution was evenly mixed.

### Synthesis of carbon dots

The precursor solution was synthesized via microwave irradiation for 50 min and 60 min to produce CDs in powder form. The powder was then dissolved in 100 mL of distilled water through stirring with a chemical spatula. The CD solution was separated from the solid material using filter paper and centrifuged at 4,000 rpm for 20 min (Architha et al. 2021). There are four types of CDs: fresh leaves microwaved for 50 min (referred to as DS 50) and 60 min (DS 60) and dried leaves microwaved for 50 min (DK 50) and 60 min (DK 60). Afterward, the leaves were stored in reagent bottles

for further use as a CR catalyst. The prepared CDs were characterized via FTIR and UV–vis spectrophotometry.

### Studies of dye degradation

The concentration of CR dye used was 5 mg/L for two different volumes of CDs: 5 mL and 10 mL. Approximately 5 mL of CDs was added to 100 mL of the dye solution. The reaction solution was placed in a sealed box for irradiation by a 300 W halogen lamp. CR dye degradation was monitored separately at different experimental parameters to test the photocatalytic performance of CDs at a maximum wavelength value of 498 nm (Zaib et al., 2021). The dye degradation rate can be calculated using Eq. (1) (Zaib et al., 2023):

$$\%D = \frac{A_0 - A}{A_0} \times 100\% \quad (1)$$

### Kinetics modeling of dye degradation

Kinetic modeling was employed to analyze the photocatalytic degradation kinetics data of synthesized CDs on CR (Mansuriya and Altintas 2021):

$$\text{Order 0 : } A = A_0 - kt \quad (2)$$

$$\text{Order 1 : } \ln A = \ln A_0 - kt \quad (3)$$

$$\text{Order 2 : } \frac{1}{A} = kt + \frac{1}{A_0} \quad (4)$$

Here,  $A_0$  and  $A$  represent the concentration of dye molecules in solution at times  $t$  and 0, respectively, and  $k$  is the appropriate rate constant.

## Results and discussion

CDs have been successfully synthesized using a carbon source from Waru (*Hibiscus Tiliaceus L.*) leaves via the MAM. The aim of this synthesis is to determine the absorption wavelength of CDs and their photocatalytic activity through the assessment of their ability to transform harmful CR into harmless compounds (clean water). The characteristics studied include absorbance spectrum, surface structure analyzed through FTIR spectra, degradation efficiency, and degradation kinetics. Figure 2 illustrates the physical appearance of the CDs under visible and UV light, the relationship between bandgap and luminescence color, and the photocatalytic mechanism of CDs.

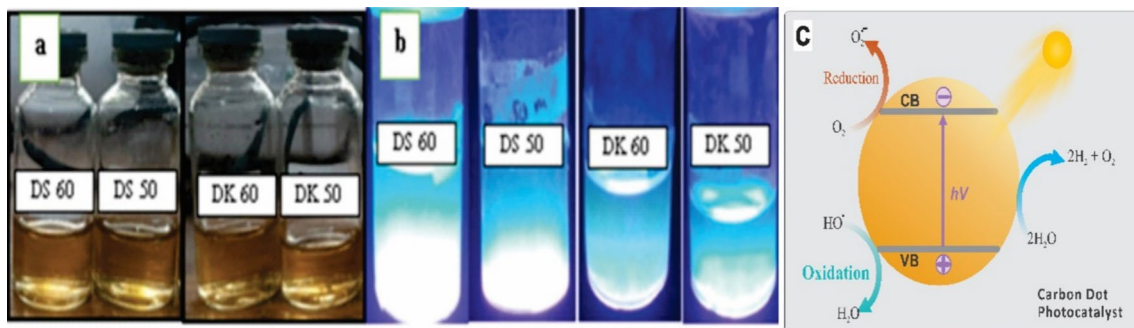


**Fig. 2** **a** Solution of CDs under visible light; **b** solution of CDs irradiated with UV light at a wavelength of 395 nm; **c** photocatalytic organic transformation from harmful organic pollution to harmless compounds

Figure 2a illustrates a solution of CDs irradiated with visible light, resulting in a brown solution, while Fig. 2(b) illustrates CDs irradiated with UV light at a wavelength of 395 nm. The CDs exhibit luminescence indicated by a blue solution. As reported by Fahri et al. (2022), a relationship exists between luminescence color and the bandgap of CDs; brown luminescence indicates a lower bandgap compared with blue luminescence. The color arises from photon emission when electrons from the CB jump to the VB for recombination, releasing their energy, which depends on the bandgap of CDs. Ozyurt et al. (2023) reported that photoluminescence (PL) properties depended on the size,  $sp^2$ -conjugated core, and functional groups on the surface electronic states of CDs. They also reported that the blue emission was due to  $sp^2$  hybridization and that the green emission was due to the electron redistribution in CD aggregation, which was affected by the surface groups being close to each other.

A comparison between Fig. 2a and b indicates that the CDs derived from Waru (*Hibiscus Tiliaceus L.*) leaves exhibit a bandgap under any source of irradiation, suggesting a high potential for photocatalyst applications. Figure 1d illustrates the mechanism of CDs as photocatalysts. In this case, the electron at the VB (referred to as highest occupied molecular orbital in (c)) gains energy from the irradiation source, allowing it to jump to the higher energy position, the CB (referred to as lowest unoccupied molecular orbital in (c)), leaving behind a hole at the VB. The electron at the CB exits the CDs to react with  $O_2$  through a reduction process, while the hole at the VB reacts with  $H_2O$  through an oxidation process. Both reaction processes produce radical atoms  $OH^\cdot$ , which are useful for breaking the bonds of the chemical structure of the pollutant until  $H_2O$  and  $CO_2$  are obtained as the final products.

### Absorption spectrum of CDs

UV–vis spectrophotometry was employed to determine the absorbance spectra of CDs as a function of wavelength. The absorbance spectrum of CDs synthesized from Waru leaves (*Hibiscus Tiliaceus L.*) is illustrated in Fig. 3.

As shown in Fig. 3, the fresh leaf-derived sample DS 50 shows two absorbance peaks at the wavelengths 322 nm and 339 nm, while sample DS 60 shows peaks at 325 nm and 332 nm. In a typical UV – vis spectrum, there are two typical absorption peaks arising from the  $\pi-\pi^*$  transition of the  $C=C$  bond and the  $n-\pi^*$  transition of the heteroatoms (e.g., N, O, P, B, S, and Se). For dried leaf-derived samples, DK 50 shows absorption peaks at 325 nm and 336 nm, while DK 60 shows peaks at 322 nm and 339 nm. These peaks correspond to the absorbance spectrum of CDs measured at a wavelength of 260–550 nm (Dewi et al. 2016) indicating the presence of  $n-\pi^*$  transitions of heteroatoms (e.g., N, O, P, B,

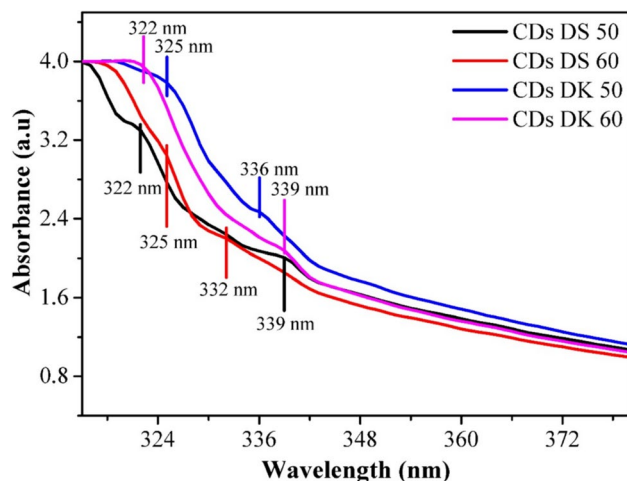


**Fig. 3** Absorption spectrum of CDs synthesized from fresh (DS) and dry (DK) Waru (*Hibiscus Tiliaceus L.*) leaves was obtained through microwave irradiation for 50 and 60 min



S, and Se) attached at the surface state of the CDs through multiple bonds, in this case C=O bonds (Sausan et al. 2021; Vikneswaran et al. 2014; Remli and Aziz 2020). There are three main possible emission sources of CDs, which depend on their structure:

1. Carbon core from polyaromatic units (Smrithi et al. 2022).
2. Surface defect states at the edge of  $sp^2$  carbon domains serve as surface trap states. The contribution from  $sp^2$  carbon generally requires a significant fraction of  $sp^2$  aromatic units (Cheng et al. 2022).
3. Molecular-like fluorophores synthesized via multi-component procedures result from amide-containing molecular-like fluorophores attached at the surface states (Bayda et al. 2021).

### FTIR spectra of CDs

FTIR spectroscopy was conducted to determine the functional groups present at the surface state of CDs. The FTIR spectra of CDs from Waru leaves (*Hibiscus Tiliaceus L.*) are illustrated in Fig. 4, with observed wavenumbers ranging from 4,000 to 500  $cm^{-1}$ .

The samples feature an absorption band at 3200–3,500  $cm^{-1}$ , indicating the presence of O–H (Dewi et al. 2016; Liu et al. 2017) and N–H bonds, which appear in the form of stretching vibrations (Xu et al. 2015; Sun et al. 2020). Peaks at 2,922  $cm^{-1}$  and 2,854  $cm^{-1}$  correspond to the formation of C–H bonds (Architha et al. 2021; Deka et al. 2019; Atchudan et al. 2018; Ma et al. 2019). Peaks at wave numbers 1,722  $cm^{-1}$  and 1,627  $cm^{-1}$ , identified as

C=O ( $n-\pi^*$ ) bonds, indicate higher graphitization levels, leading to higher absorption at the CD surface (Deka et al. 2019; Bayat et al. 2019; Monte-Filho et al. 2019). A C=C ( $\pi-\pi^*$ ) bond is also formed at 1,523  $cm^{-1}$  (Bayat et al. 2019). Overall, the functional groups formed are influenced by the stretching vibration in the core and at the surface state (Sun et al. 2021).

The absorption capacity of CDs is due to the complex nature of the surface state CD structures, and little progress has been reported so far in determining the position of the ground- or excited-state energy levels (Xu et al. 2020). The intriguing absorption properties of CDs have attracted significant research attention for photocatalyst applications (Zhang et al. 2020). CDs typically exhibit excitation wavelength-dependent emission or absorption properties, which are influenced by the nanocrystal size and affect their energy band gap. Typically, existing nonradiative recombination occurs when the fluorescence of CDs is low, indicating a low band gap (Wang and Lu 2022). Carbon, nitrogen, hydrogen, and oxygen bonds are affected by the surface state structure of CDs. The presence of nitrogen and hydrogen bonds impacts the band gap, as nitrogen can create new energy levels, particularly at the surface state of CDs (Tuerhong et al. 2017).

### Analysis of CR degradation by CDs

In this study, the photocatalytic activity of CDs derived from Waru leaves (*Hibiscus Tiliaceus L.*) was assessed according to the photodegradation of CR dye under irradiation using a 300 W halogen lamp for up to 90 min. Two volumes of CDs, namely 5 mL and 10 mL, were added to 100 mL of CR solution with a concentration of 5 mg/L (Zaib et al., 2023). UV–vis spectrophotometry was employed to record the absorbance spectrum during irradiation, and the spectra are presented in Fig. 5. The degradation of the CR solution, as evidenced by a decrease in the absorption peak during irradiation, indicates that CDs are functioning as a photocatalyst (Bie et al. 2022).

Photocatalysts can function in the liquid or gas phase through a three-stage photodegradation process: diffusion, absorbance, and desorption (Petit et al. 2016). The diffusion process occurs before irradiation, in which the surface state of CDs plays a crucial role. A larger surface area results in higher diffusion efficiency. Furthermore, the absorption process involves electron transfer between the hydroxyl carbon of CR and the atoms at the surface state of CDs. In this study, the sample underwent continuous irradiation or energy addition for up to 90 min. Finally, the desorption process releases back the ions that were used to break the chemical bonds of harmful CR, resulting in harmless byproducts (Indira et al. 2021).

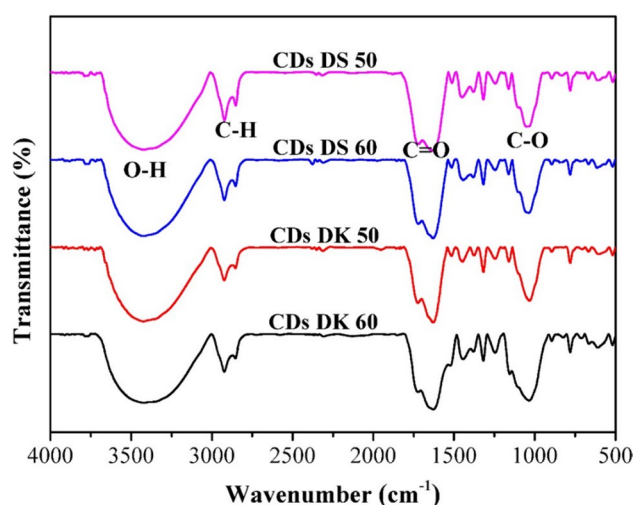


**Fig. 4** FTIR spectra of CDs synthesized from fresh (DS) and dry (DK) Waru (*Hibiscus Tiliaceus L.*) leaves, prepared via microwave irradiation for 50 and 60 min

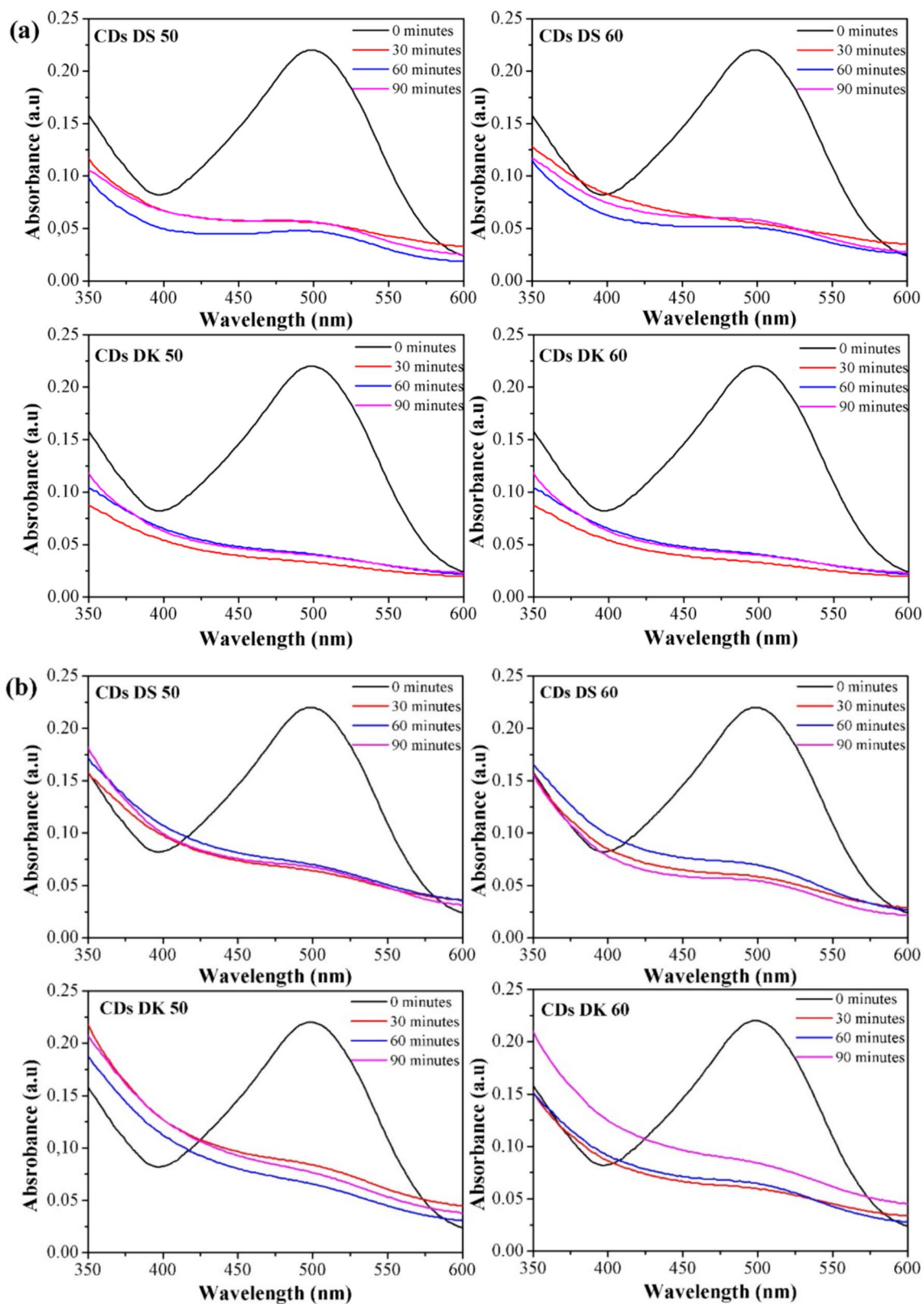


Fig. 5 UV-vis absorption spectra depicting the photocatalytic degradation of CR in the presence of CDs a for 5 mL CDs and b for 10 mL CDs

Figure 5 illustrates the percentage of photocatalytic CR degradation based on Eq. (1), and the corresponding results are presented in Table 1. DK 60 exhibits the highest degradation efficiency (87%), with irradiation times of 30 min and 90 min for 10 mL CDs in CR solutions.

The degradation test was conducted under different irradiation times ranging from 0 to 90 min for CD volumes of 5 mL and 10 mL. CR degradation increased steadily with increasing irradiation time owing to electrostatic interactions between the catalyst surface and the dye ions of CR (Arul and Sethuraman 2018). For the other CDs, the degradation rate first increased and then decreased owing to competition between reactants and products. The low degradation rate of dyes after a certain time limit was due to the short lifetime of the photocatalyst owing to the deactivation of reactive species (Zaib et al., 2021). The CR degradation efficiencies in this study are shown in Table 2, and a comparison among

various carbon sources and pollutant types is presented in Table 3.

According to Table 3, various CDs were applied as photocatalysts for dyes such as methylene blue (MB), methylene orange (MO), and CR, with specified irradiation times. The degradation process of dyes after a specific time is influenced by the short lifespan of the photocatalyst owing to the deactivation of reactive species (Zaib et al., 2021). A comparison with various references in Table 3 demonstrates the high potential of the CDs synthesized in this study as a photocatalyst. For example, the CDs achieve a CR degradation efficiency of 87% in just 30 min, indicating that the surface state of CDs from Waru leaves is highly active in bonding with CR atoms, leading to a high generation of electrons and holes for producing radicals. In contrast, coffee grounds, watermelon rinds, and olive oils require a minimum of 2 h to degrade MO or MB (Maddu et al. 2020; Remli and Aziz 2020; Sawalha et al. 2021).

The kinetic parameters of the three models and their correlation coefficients were calculated for different volumes of CDs with CR concentrations of 5 mg/L. The rate constants ( $k$ ) are shown in Table 4, with subscript numbers corresponding to orders 0, 1, and 2.

According to Eq. (2), the order kinetic model was assessed by plotting Fig. 6, which depicts the  $A - A_0$  relationship at different irradiation times for CR on different CDs. Similarly, for Eq. (3),  $\ln A$  and  $\frac{1}{A}$  (Eq. 4) were plotted to indicate the corresponding relationships at different irradiation times.

According to Fig. 6, the degradation rate constant ( $k$ ) and the correlation coefficient ( $R^2$ ) were determined for each type of CD (Zaib et al., 2023), and the results are summarized in Table 4. The rate constants for fresh leaf-derived CDs DS 60 with a volume of 5 mL are as follows: order 0 ( $k_0$ )  $0.0016 \text{ min}^{-1}$ , order 1 ( $k_1$ )  $0.0133 \text{ min}^{-1}$  and order 2 ( $k_2$ )  $0.1290 \text{ min}^{-1}$ . These values are greater than those for dry leaf-derived CDs DK 60 with a volume of 5 mL, which are

**Table 2** CR degradation performance of different volumes of CDs (5 mL and 10 mL)

Sample	Irradiation time (min)	Degradation (%)	
		5 mL CDs	10 mL CDs
CDs DS 50	30	71	75
	60	69	78
	90	68	75
CDs DS 60	30	73	75
	60	68	77
	90	75	73
CDs DK 50	30	61	85
	60	65	81
	90	70	81
CDs DK 60	30	72	87
	60	71	82
	90	61	87

**Table 3** CD-based photocatalysts for various carbon sources, dye types, and their irradiation times and degradation efficiencies

Catalyst	Carbon Source	Pollutant	Light Source	Time (min)/ Degradation (%)	Refs.
–	N-CDs	<i>Actinidia deliciosa</i>	UV-vis	10/N(A)	(Arul and Sethuraman 2018)
–	N-CDs	<i>Citrus grandis</i>	Sunlight	90/N(A)	(Ramar et al. 2018)
–	–	Dragon fruit	UV-vis	6.5/N(A)	(Arul et al. 2017)
CDs	–	<i>Elettaria cardamomum</i> leaves	Halogen 300 W	55 and 50/N(A)	(Zaib et al., 2021)
CDs	–	<i>Polyalthia longifolia</i> leaves	Halogen 100 W	60 and 90/N(A)	(Zaib et al., 2023)
–	ZnO/CDs	Coffee grounds	UV	150/80.34	(Maddu et al. 2020)
–	N-CDs	<i>Averrhoa carambola</i>	UV	2/99	(Zulfajri et al. 2019)
CDs	–	Watermelon rinds	Halogen 500 W	120/68.941	(Remli and Aziz 2020)
CDs	–	Olive oil	Lamp 50 W	120/92	(Sawalha et al. 2021)
–	N-CDs	Sprout of <i>Borassus flabellifer</i>	UV-vis	120/ N(A)	(Arul et al. 2020)





**Table 4** CD kinetic rate ( $k$ ), with subscript numbers corresponding to the order 0, order 1, and order 2

Sample	$k_0$ ( $\text{min}^{-1}$ )		$k_1$ ( $\text{min}^{-1}$ )		$k_2$ ( $\text{min}^{-1}$ )		
	5 mL	10 mL	5 mL	10 mL	5 mL	10 mL	
1	CDs DS 50	0.0015	0.0017	0.0111	0.0143	0.0929	0.1459
2	CDs DS 60	0.0016	0.0016	0.0133	0.0135	0.1290	0.1314
3	CDs DK 50	0.0016	0.0018	0.0124	0.0163	0.1112	0.1862
4	CDs DK 60	0.0013	0.0015	0.0093	0.0112	0.0693	0.0747

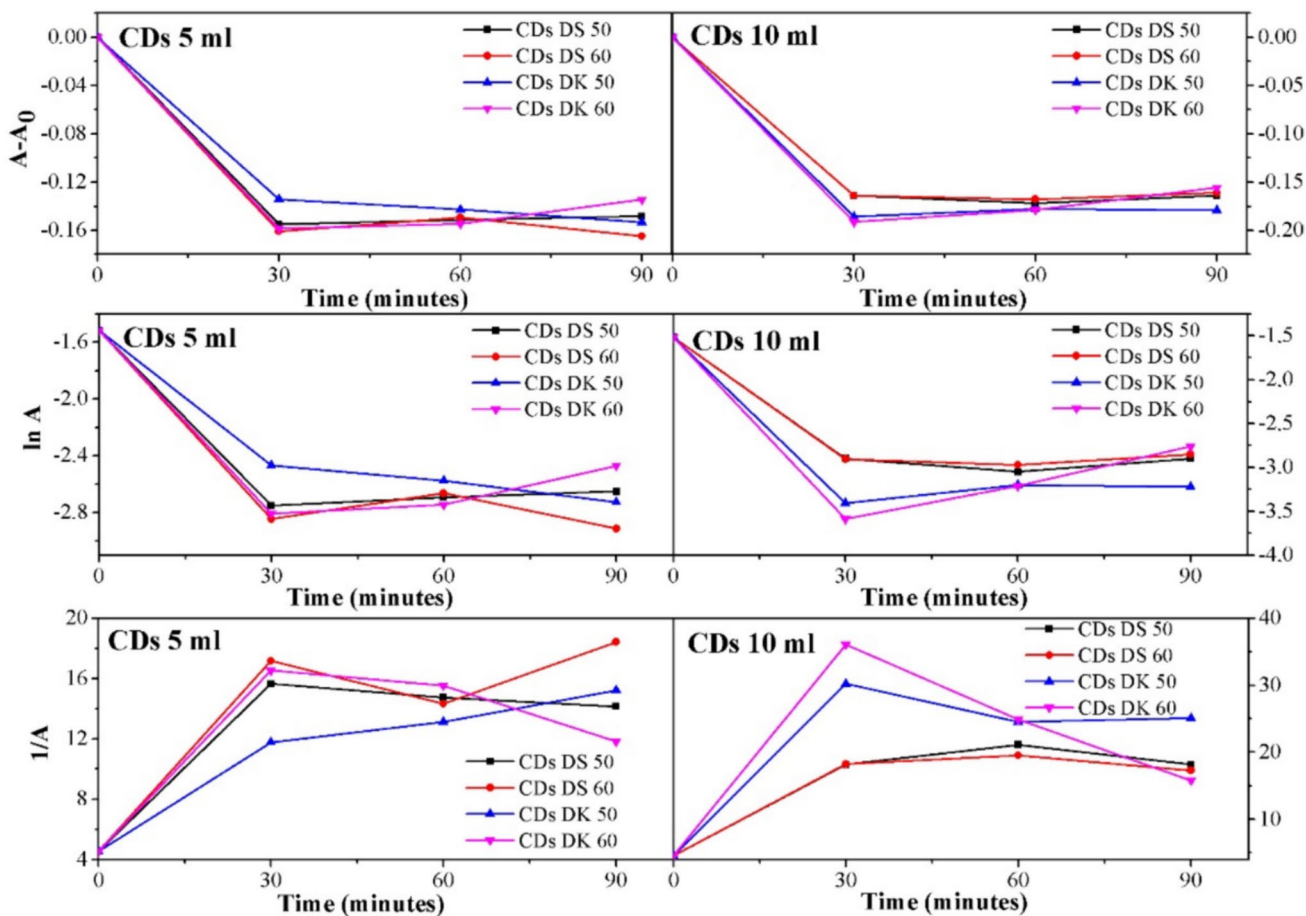


**Fig. 6** Kinetics for the degradation of CR dye by CDs photocatalyst. for 5 mL CDs and 10 mL CDs derived from Fig. 4

as follows: order 0 ( $k_0$ )  $0.0013 \text{ min}^{-1}$ , order 1 ( $k_1$ )  $0.0093 \text{ min}^{-1}$  and order 2 ( $k_2$ )  $0.0693 \text{ min}^{-1}$ . Thus, the degradation rate constant ( $k$ ) for DS 60 with a volume of 5 mL is greater than that for CDs 60 with the same volume. This occurs because degradation increases with different irradiation times, and the value of  $k$  is obtained from the slope of the plot in Fig. 6.

According to Fig. 6 and Table 4, DS 60 with a volume of 5 mL photocatalytically degrades CR within 90 min of irradiation, while DK 60 degrades CR within only 30 min of irradiation.

For DK 60, degradation increased rapidly in the first 30 min of irradiation exposure owing to the slow degradation of the dye after a specific time, likely due to the short lifetime of the photocatalyst and the deactivation of reactive oxygen species (Zaib et al., 2021; Zaib et al., 2023). Molecules probably act as a barrier to visible light, thereby reducing the concentration of  $\text{OH}^-$  ions and slowing down the dye degradation process. However, for DS 60, the opposite occurs, leading to an increase in the production of  $\text{OH}^-$  radicals and consequently an increase in the degradation rate.

## Conclusion

According to the results of the research, data analysis, and discussion, CDs derived from Waru leaves (*Hibiscus Tiliaceus L.*) exhibit an absorbance peak at wavelengths of 300 nm to 340 nm, consistent with the absorbance spectrum of CDs within the wavelength range of 260 nm to 550 nm. The CDs derived from Waru leaves demonstrate photocatalytic activity in degrading CR. This is evidenced by the maximum degradation rates achieved, with the fresh leaf-derived CDs DS 60 achieving 75% degradation after 90 min of irradiation, and the dry leaf-derived CDs DK 60 achieving 87% degradation after 30 min of irradiation.

**Acknowledgements** Thanks to Lab. Material and Energy is responsible for supporting the research facility, and Mr. Ardiansyah is accountable for the helpful discussion in analyzing the data.

**Author's contribution** All authors contributed to the study's conception and design. Literature search, data collection, and analysis were performed by NAH, BA, and DT. The first draft of the manuscript was written by NAH, and all authors commented on previous versions. All authors read and approved the final manuscript: conceptualization idea, review and editing, supervision by DT.

**Funding** The authors declare that no funds, grants, or other support were received during the preparation of this manuscript.

**Data availability** All data generated or analyzed during this study are included in this published article.

## Declarations

**Conflict of interest** The authors declare that they have no known competing financial interests or personal relationships that could have appeared to influence the work reported in this paper.

**Ethics approval** Not applicable.

**Consent to participate** Not applicable.

**Consent for publication** All authors mutually agree that the manuscript can be submitted to International Journal of Environmental Science and Technology.

## References

- Aliah H, Aji MP, Sustini E, Budiman M, Abdullah M (2012) TiO<sub>2</sub> nanoparticles-coated polypropylene copolymer as photocatalyst on methylene blue photodegradation under solar exposure. *Am J Environ Sci* 8:280–290. <https://doi.org/10.3844/ajessp.2012.280.290>
- Andriani Y, Mohamad H, Bhupalan K, Abdullah MI, Amir H (2017) Phytochemical analyses, antibacterial and anti-biofilm activities of mangrove-associated *Hibiscus tiliaceus* extracts and fractions against *Pseudomonas aeruginosa*. *J Sustain Sci Manag* 12:45–51
- Architha N, Ragupathi M, Shobana C, Selvankumar T, Kumar P, Lee YS, Kalai Selvan R (2021) Microwave-assisted green synthesis of fluorescent carbon quantum dots from Mexican Mint extract for Fe<sup>3+</sup> detection and bio-imaging applications. *Environ Res* 199:111263. <https://doi.org/10.1016/j.envres.2021.111263>
- Arul V, Chandrasekaran P, Sethuraman MG (2020) Reduction of Congo red using nitrogen doped fluorescent carbon nanodots obtained from sprout extract of *Borassus flabellifer*. *Chem Phys Lett* 754:137646. <https://doi.org/10.1016/j.cplett.2020.137646>
- Arul V, Edison TNJI, Lee YR, Sethuraman MG (2017) Biological and catalytic applications of green synthesized fluorescent N-doped carbon dots using *Hylocereus undatus*. *J Photochem Photobiol b Elsevier* 168:142–148. <https://doi.org/10.1016/j.jphotobiol.2017.02.007>
- Arul V, Sethuraman MG (2018) Facile green synthesis of fluorescent N-doped carbon dots from *Actinidia deliciosa* and their catalytic activity and cytotoxicity applications. *Opt Mater (amst)* 78:181–190. <https://doi.org/10.1016/j.optmat.2018.02.029>
- Atchudan R, Edison TNJI, Aseer KR, Perumal S, Lee YR (2018) Hydrothermal conversion of *Magnolia liliiflora* into nitrogen-doped carbon dots as an effective turn-off fluorescence sensing, multi-colour cell imaging and fluorescent ink. *Colloids Surf B Biointerfaces* 169:321–328. <https://doi.org/10.1016/j.colsurfb.2018.05.032>
- Atchudan R, Edison JI, Shanmugam TN, Perumal M, Somanathan S, Lee T (2021) Sustainable synthesis of carbon quantum dots from banana peel waste using hydrothermal process for in vivo bioimaging. *Phys Low Dimens Syst Nanostruct* 126:114417. <https://doi.org/10.1016/j.physe.2020.114417>
- Bayat A, Masoum S, Hosseini ES (2019) Natural plant precursor for the facile and eco-friendly synthesis of carbon nanodots with multifunctional aspects. *J Mol Liq* 281:134–140. <https://doi.org/10.1016/j.molliq.2019.02.074>
- Bayda S, Amadio E, Cailotto S, Frión-Herrera Y, Perosa A, Rizzolio F (2021) Carbon dots for cancer nanomedicine: a bright future. *Nanoscale Adv* 3:5183–5221. <https://doi.org/10.1039/D1NA00036E>
- Bie C, Zhu B, Wang L, Yu H, Jiang C, Chen T, Yu J (2022) A bifunctional CdS/MoO<sub>2</sub>/MoS<sub>2</sub> catalyst enhances photocatalytic H<sub>2</sub> evolution and pyruvic acid synthesis. *Angew Chem Int Ed Engl* 61:e202212045. <https://doi.org/10.1002/anie.202212045>
- Cheng Y-Z, Ji W, Wu X, Ding X, Liu X-F, Han B-H (2022) Persistent radical cation sp<sup>2</sup> carbon-covalent organic framework for photocatalytic oxidative organic transformations. *Appl Catal B* 306:121110. <https://doi.org/10.1016/j.apcatb.2022.121110>
- Deka MJ, Dutta P, Sarma S, Medhi OK, Talukdar NC, Chowdhury D (2019) Carbon dots derived from water hyacinth and their application as a sensor for pretilachlor. *Heliyon* 5:e01985. <https://doi.org/10.1016/j.heliyon.2019.e01985>
- Dewi ARC, Aji MP, Sulhadi S (2016) Absorbance spectrum carbon nanodots (C-dots) Daun tembakau. In: *Prosiding seminar nasional fisika (e-Journal)* 5, SNF2016-MPS. <https://doi.org/10.21009/0305020225>
- Fahri AN, Ilyas S, Anugrah MA, Heryanto H, Azlan M, Ola ATT, Rahmat R, Yudasari N, Tahir D (2022) Bifunctional purposes of composite TiO<sub>2</sub>/CuO/carbon dots (CDs): Faster photodegradation pesticide wastewater and high performance electromagnetic wave absorber. *Materialia* 26:101588. <https://doi.org/10.1016/j.mtla.2022.101588>
- Gu D, Shang S, Yu Q, Shen J (2016) Green synthesis of nitrogen-doped carbon dots from lotus root for Hg(II) ions detection and cell imaging. *Appl Surf Sci* 390:38–42. <https://doi.org/10.1016/j.apsusc.2016.08.012>
- Haryono H, Faizal D, M, Liamita NC, Rostika A (2018) Pengolahan limbah Zat Warna tekstil Terdispersi dengan metode wlektroflotasi. *EduChemia (Jurnal Kimia dan Pendidikan)* 3:94. <https://doi.org/10.30870/educhemia.v3i1.2625>



- Indira K, Shanmugam S, Hari A, Vasantharaj S, Sathiyavimal S, Brindhadevi K, El Askary A, Elfasakhany A, Pugazhendhi A (2021) Photocatalytic degradation of Congo red dye using nickel–titanium dioxide nanoflakes synthesized by Mukia madrasapatna leaf extract. *Environ Res* 202:111647. <https://doi.org/10.1016/j.envres.2021.111647>
- Januariawan W, Wayan I, Suyasa B, Gunawan G (2019) Biodegradasi Congo red menggunakan biofilm Yang Ditumbuhkan dengan Inokulum suspensi aktif pada permukaan batu vulkanik. *Cakra Kimia (Indonesian e J Appl Chem)* 7:36–45
- Kumbhar S, De M (2023) Waste biomass derived nitrogen-rich carbon dots augmented g-C<sub>3</sub>N<sub>4</sub> photocatalyst for valorization of glycerol. *Mater Sci Eng B* 298:116815. <https://doi.org/10.1016/j.mseb.2023.116815>
- Liu W, Diao H, Chang H, Wang H, Li T, Wei W (2017) Green synthesis of carbon dots from rose-heart radish and application for Fe<sup>3+</sup> detection and cell imaging. *Sens Actuators B* 241:190–198. <https://doi.org/10.1016/j.snb.2016.10.068>
- Ma X, Li S, Hessel V, Lin L, Meskers S, Gallucci F (2019) Synthesis of luminescent carbon quantum dots by microplasma process. *Chem Eng Process Intensif* 140:29–35. <https://doi.org/10.1016/j.cep.2019.04.017>
- Maddu A, Meliafatmah R, Rustami E (2020) Enhancing photocatalytic degradation of methylene blue using znO/carbon dots nanocomposite derived from coffee grounds. *Pol J Environ Stud* 30:273–282. <https://doi.org/10.15244/pjoes/120156>
- Mansuriya BD, Altintas Z (2021) Carbon dots: Classification, properties, synthesis, characterization, and applications in health care—an updated review (2018–2021). *Nanomaterials (Basel)* 11. <https://doi.org/10.3390/nano11102525>
- Mondal TK, Mondal S, Ghorai UK, Saha SK (2019) White light emitting lanthanide based carbon quantum dots as toxic Cr (VI) and pH sensor. *J Colloid Interface Sci* 553:177–185. <https://doi.org/10.1016/j.jcis.2019.06.009>
- Monte-Filho SS, Andrade SIE, Lima MB, Araujo MCU (2019) Synthesis of highly fluorescent carbon dots from lemon and onion juices for determination of riboflavin in multivitamin/mineral supplements. *J Pharm Anal* 9:209–216. <https://doi.org/10.1016/j.jpha.2019.02.003>
- Nasrollahzadeh M, Issaabadi Z, Sajadi SM (2018) Green synthesis of Pd/Fe<sub>3</sub>O<sub>4</sub> nanocomposite using Hibiscus tiliaceus L. extract and its application for reductive catalysis of Cr(VI) and nitro compounds. *Sep Purif Technol* 197:253–260. <https://doi.org/10.1016/j.seppur.2018.01.010>
- Ozyurt D, Al Kobaisi MA, Hocking RK, Fox B (2023) Properties, synthesis, and applications of carbon dots: a review. *Carbon Trends* 12:100276. <https://doi.org/10.1016/j.cartre.2023.100276>
- Petit M, Michez L, Raimundo J-M, Malinowski T, Dumas P (2016) An introduction to photocatalysis through methylene blue photodegradation. *Eur J Phys* 37:1–11. <https://doi.org/10.1088/0143-0807/37/6/065808>
- Pires NR, Santos CMW, Sousa RR, De Paula RCM, Cunha PLR, Feitosa JPA (2015) el and fast microwave-assisted synthesis of carbon quantum dots from raw cashew gum. *J Braz Chem Soc* 26:1274–1282. <https://doi.org/10.5935/0103-5053.20150094>
- Ramar V, Moothattu S, Balasubramanian K (2018) Metal free, sunlight and white light based photocatalysis using carbon quantum dots from Citrus grandis: A green way to remove pollution. *Sol Energy* 169:120–127. <https://doi.org/10.1016/j.solener.2018.04.040>
- Rawool PP, Parulekar BC (2019) Phytochemical screening of Hibiscus tiliaceus by FTIR spectroscopic analysis. *Int J Pharm Biol Sci* 9:1308–1319
- Remli URRP, Aziz AA (2020) Photocatalytic degradation of methyl orange using carbon quantum dots (CQDs) derived from watermelon rinds. *IOP Conf Ser Mater Sci Eng* 736. <https://doi.org/10.1088/1757-899X/736/4/042038>
- Saraswati I, Diantariani N, Suarya P (2015) Fotodegradasi zat Warna tekstil Congo red dengan Fotokatalis ZnO-Arang aktif Dan Sinar ultraviolet (Uv). *J Kimia* 9:175–182
- Sausan FW, Puspitasari AR, Yanuarita PD (2021) Studi Literatur pengolahan Warna pada limbah Cair industri tekstil menggunakan metode proses adsorpsi, filtrasi, dan elektrolisis. *J Tecnosienza* 5:213. <https://doi.org/10.51158/tecnosienza.v5i2.427>
- Sawalha S, Azzam H, Bin Ali R, Dweikat H, Anaya K (2021) Photodegradation of methylene blue by carbon nanodots synthesized from olive solid wastes. In: Proceedings of the 9th Jordan international chemical engineering conference (JICHEC9) 14
- Simsek S, Ozge Alas M, Ozbek B, Genc R (2019) Evaluation of the physical properties of fluorescent carbon nanodots synthesized using nerium oleander extracts by microwave-assisted synthesis methods. *J Mater Res Technol* 8:2721–2731. <https://doi.org/10.1016/j.jmrt.2019.04.008>
- Smrithi SP, Kottam N, Vergis BR (2022) Heteroatom modified hybrid carbon quantum dots derived from Cucurbita pepo for the visible light driven photocatalytic dye degradation. *Top Catal*. <https://doi.org/10.1007/s11244-022-01581-x>
- Suhail B, Bajpai SK, Souza AD (2022) ‘Microwave assisted facile green synthesis of carrageenan carbon dots(CDs) and their interaction with Hibiscus Rosa sinensis leaf cells. *Int J Environ Anal Chem* 102:2697–2713. <https://doi.org/10.1080/03067319.2020.1759563>
- Sun D, Liu T, Wang C, Yang L, Yang S, Zhuo K (2020) Hydrothermal synthesis of fluorescent carbon dots from gardenia fruit for sensitive on-off-on detection of Hg<sub>2</sub><sup>+</sup> and cysteine. *Spectrochim Acta A Mol Biomol Spectrosc* 240:118598. <https://doi.org/10.1016/j.saa.2020.118598>
- Sun R, Wang Y, Zhang Z, Qu Y, Li Z, Li B, Wu H, Hua X, Zhang S, Zhang F, Jing L (2021) Ultrathin phosphate-modulated zinc phthalocyanine/perylene diimide supermolecule Z-scheme heterojunctions as efficiently wide visible-light photocatalysts for CO<sub>2</sub> conversion. *Chem Eng J* 426:131266. <https://doi.org/10.1016/j.cej.2021.131266>
- Tuerhong M, Xu Y, Yin X-B (2017) Review on carbon dots and their applications. *Chin J Anal Chem* 45:139–150. [https://doi.org/10.1016/S1872-2040\(16\)60990-8](https://doi.org/10.1016/S1872-2040(16)60990-8)
- Vikneswaran R, Ramesh S, Yahya R (2014) Green synthesized carbon nanodots as a fluorescent probe for selective and sensitive detection of iron(III) ions. *Mater Lett* 136:179–182. <https://doi.org/10.1016/j.matlet.2014.08.063>
- Wang B, Lu S (2022) The light of carbon dots: From mechanism to applications. *Matter* 5:110–149. <https://doi.org/10.1016/j.matt.2021.10.016>
- Widiyandari H, Prilita O, Al Ja'farawy, M.S., Nurosyid, F., Arutanti, O., Astuti, Y., Mufti, N., (2023) Nitrogen-doped carbon quantum dots supported zinc oxide (ZnO/N-CQD) nanoflower photocatalyst for methylene blue photodegradation. *Results Eng* 17:100814. <https://doi.org/10.1016/j.rineng.2022.100814>
- Xu A, Wang G, Li Y, Dong H, Yang S, He P, Ding G (2020) Carbon-based quantum dots with solid-state photoluminescent: Mechanism, implementation, and application. *Small* 16:e2004621. <https://doi.org/10.1002/sml.202004621>
- Xu J, Lai T, Feng Z, Weng X, Huang C (2015) Formation of fluorescent carbon nanodots from kitchen wastes and their application for detection of Fe(3.). *Luminescence* 30:420–424. <https://doi.org/10.1002/bio.2754>
- Yang X, Wang D, Luo N, Feng M, Peng X, Liao X (2020) Green synthesis of fluorescent N, S-carbon dots from bamboo leaf and the interaction with nitrophenol compounds. *Spectrochim Acta a: Mol Biomol Spectrosc* 239:118462. <https://doi.org/10.1016/j.saa.2020.118462>
- Zaib M, Akhtar A, Maqsood F, Shahzadi T (2021) Green synthesis of carbon dots and their application as photocatalyst in dye



degradation studies. Arab J Sci Eng 46:437–446. <https://doi.org/10.1007/s13369-020-04904-w>

Zaib M, Arshad A, Khalid S, Shahzadi T (2023) One pot ultrasonic plant mediated green synthesis of carbon dots and their application invisible light induced dye photocatalytic studies: a kinetic approach. Int J Environ Anal Chem 103:5063–5081. <https://doi.org/10.1080/03067319.2021.1934463>

Zhang Z, Yi G, Li P, Zhang X, Fan H, Zhang Y, Wang X, Zhang C (2020) A minireview on doped carbon dots for photocatalytic and electrocatalytic applications. Nanoscale 12:13899–13906. <https://doi.org/10.1039/D0NR03163A>

Zulfajri M, Dayalan S, Li W-Y, Chang C-J, Chang Y-P, Huang GG (2019) Nitrogen-doped carbon dots from Averrhoa carambola fruit extract as a fluorescent probe for methyl orange. Sensors (Switzerland) 19. <https://doi.org/10.3390/s19225008>

Springer Nature or its licensor (e.g. a society or other partner) holds exclusive rights to this article under a publishing agreement with the author(s) or other rightsholder(s); author self-archiving of the accepted manuscript version of this article is solely governed by the terms of such publishing agreement and applicable law.

